A Robust Image Watermarking Scheme Using Local Statistical Distribution in the Contourlet Domain

Hamidreza Sadreazami, *Member, IEEE*, and Marzieh Amini, *Member, IEEE*

***Abstract*—Data security is a main concern in everyday data transmissions in the Internet. A possible solution to guarantee a secure and legitimate transaction is via hiding a piece of tractable information into the multimedia signal, i.e., watermarking. This brief proposes a new multiplicative image watermarking scheme in the contourlet domain by taking into account the local statistical properties and inter-scale dependencies of the contourlet coefficients of images. Although the contourlet coefficients are non-Gaussian within a sub-band, their local distribution fits the Gaussian distribution very well. In addition, it is known that there exist across-scale dependencies among these coefficients. In view of this, we propose the use of bivariate Gaussian (BVG) distribution to model the distribution of the contourlet coefficients. Motivated by the modeling results, an optimum blind watermark decoder is designed in the contourlet domain using the maximum likelihood method. By means of carrying out a number of experiments, the performance of the proposed decoder is investigated with regard to the bit error rate and compared to other decoders. It will be shown that the proposed decoder built upon the BVG model is superior to other decoders in terms of rate of error. It will also be shown that the proposed decoder provides higher robustness in comparison to other decoders in presence of attacks such as filtering, compression, cropping, scaling, and noise.**

***Index Terms*—Digital image watermarking, extraction, bivariate Gaussian model, contourlet domain.**

I. Introduction

DIGITAL watermarking has been used in copyright protection and content authentication of images in multimedia. Watermarking techniques may be classified based on the embedding domain, embedding approach, and extraction or detection methods [1], [2]. Watermark embedding is performed either in spatial or spectral domain using additive, multiplicative or quantization-based [21] approaches. The extraction or detection method can be blind or non-blind. It is known that the multiplicative embedding approach provides more robustness than the additive one [3]. Thus, detection and extraction of the multiplicative watermarks have widely been studied [1]–[6].

Manuscript received April 5, 2018; revised June 4, 2018; accepted June 9, 2018. Date of publication June 12, 2018; date of current version December 20, 2018. This brief was recommended by Associate Editor L.-P. Chau. *(Corresponding author: Hamidreza Sadreazami.)*

H. Sadreazami is with the School of Electrical Engineering and Computer Science, University of Ottawa, Ottawa, ON K1N 6N5, Canada (e-mail: hsadreaz@uottawa.ca).

M. Amini is with the Department of Electrical and Computer Engineering, McGill University, Montreal, QC H3A 0E9, Canada (e-mail: marzieh.amini@mcgill.ca).

Color versions of one or more of the figures in this paper are available online at http://ieeexplore.ieee.org.

Digital Object Identifier 10.1109/TCSII.2018.2846547

It is known that development of a blind watermark decoder needs an accurate statistical characterization of images. Recently, the statistical analysis has been conducted mostly in the sparse domain. This is due to the fact that when the watermark is embedded in the sparse domain, its robustness can significantly be increased [4], [5]. Various watermarking schemes have so far been developed, where the hidden message is embedded into the contourlet coefficients of an image, since the contourlet-domain watermarking techniques are more robust against distortions than the other sparse domain algorithms [1], [6]. In view of this, statistics of the contourlet coefficients of images have been investigated and shown to be non-Gaussian and heavy-tailed [1], [3], [6]. In addition, these coefficients have been assumed to be independent and identically distributed by the generalized Gaussian (GG) [3], Cauchy [1], K-Bessel function [10], and normal inverse Gaussian distributions [2]. However, these models have been established for the marginal distribution of the contourlet coefficients within a subband and ignored both the local distribution and inter-scale relation between the coefficients. It is noted that the local distribution of the contourlet coefficients has been shown to follow the Gaussian probability density function (PDF) rather than a non-Gaussian PDF [11]. Taking this into account, the use of the bivariate Gaussian model is proposed to characterize the local statistical properties of the contourlet coefficients as well as their inter-scale dependencies, i.e., parent and children relationship. Incorporating these statistics, a novel blind watermark decoder in the contourlet domain is designed. The proposed decoder is developed employing the bivariate Gaussian model in a maximum likelihood sense. The performance of the proposed decoder is evaluated by conducting experiments and comparing it to those of the other decoders. The proposed decoder is also examined for its robustness when undergoing various distortions.

II. Local Modeling of Images

A prevalent assumption in employing different distributions to model the coefficients of images in the frequency domain is the independent and identically distributed (i.i.d.) nature of these coefficients [3]. However, the contourlet coefficients of images have shown across scale dependencies between parent and children [12], which plays a key role in modeling these coefficients. As a consequence of which, the contourlet coefficients of the entire subband may not be assumed to be i.i.d. Thus, in order to incorporate the intra-scale dependency of such coefficients, they are locally modeled as i.i.d. Gaussian

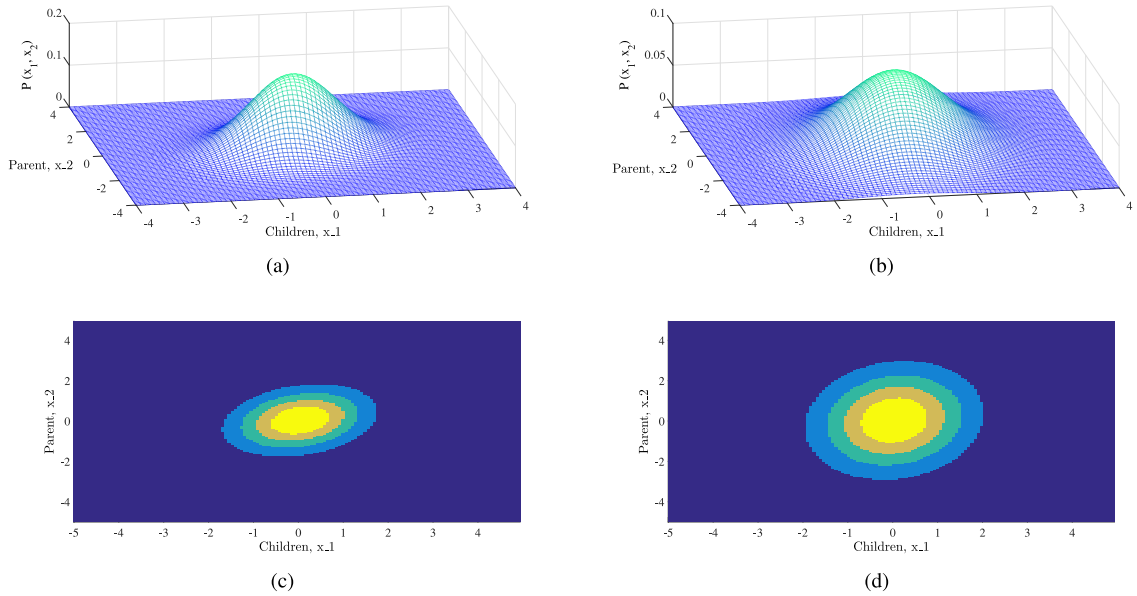

Fig. 1. Empirical joint probability distribution of contourlet coefficients and their contour representations for test images, (a)-(c) *Peppers*, and (b)-(d) *Barbara*.

distribution with conditional mean and variance. This choice is inspired by the work done in [11]. It has been shown in [11] that the local distribution of the contourlet coefficients of an image is Gaussian. In light of the above, in this brief, the use of the bivariate Gaussian (BVG) model is proposed to not only capture the local marginal distribution of the contourlet coefficients, but to consider their dependencies across scales. Fig. 1 depicts the empirical joint probability density function of the children coefficients in the finest scale and its corresponding parent in the second finest scale for two of the test images, namely, *Peppers* and *Barbara*, as well as their contour representations. It is seen from this figure that there is a significant inter-scale dependency between the contourlet coefficients in a local neighborhood, as evidenced by the contour representation of the joint distribution, which is nearly elliptic [13], and thus, can be well modeled by the bivariate Gaussian density function which is elliptic in nature when a dependency exists between two random processes [13]. In view of this, the BVG model can be used to characterize the contourlet coefficients in a local region and across scales. The zero-mean BVG probability density function is expressed as

$$P_{BVG}(x_i, x_j) = \frac{1}{2\pi\sigma_i\sigma_j\sqrt{1-\rho^2}} \exp\left[\frac{-1}{2(1-\rho^2)}\left\{\frac{x_i^2}{\sigma_i^2} + \frac{x_j^2}{\sigma_j^2} - 2\rho\frac{x_i}{\sigma_i}\frac{x_j}{\sigma_j}\right\}\right], \tag{1}$$

where x_i and x_j are children and parent coefficients in two consecutive scales, respectively, σ_i and σ_j are their standard deviations, and $-1 < \rho < 1$ is the correlation coefficient between parent and children, which is given by

$$\rho = \frac{E\{x_i x_j\}}{\sqrt{E\{x_i^2\}E\{x_j^2\}}}, \tag{2}$$

where $E\{.\}$ denotes the expectation operation.

III. Proposed Watermarking Scheme

The proposed scheme comprises of two stages; hiding the watermark message into the host image and extracting them from the received marked image. In the following, the two stages are presented.

A. Watermark Embedding

The process of inserting the hidden message bits into the host image is started by segmenting the image into several non-overlapping blocks. More specifically, the image $I(m, n)$ of size $M \times M$ is segmented into B blocks, each having size of $Q \times Q$ as

$$I(m, n) = \bigcup_{b=1}^{B} I_b(\acute{m}, \acute{n}), \tag{3}$$

where $I_b(\acute{m}, \acute{n})$ denotes one of the non-overlapping blocks, $1 < \acute{m}, \acute{n} < Q$ and $B = \frac{M^2}{Q^2}$. In order to insert a hidden message of length k bits into the image, the variance of each block is obtained and k blocks with the highest variance are selected. Each selected block is then decomposed into J scales and D directional subbands by using the multi-scale and multi-directional contourlet transform and subbands are denoted as S_{jd}, where $j = 1, \ldots, J$ and $d = 1, \ldots, D$. To promise the invisibility of the watermark, the directional subband in the finest scale having the highest energy is selected for inserting the watermark bits. The watermark bits are embedded according to the multiplicative spread spectrum rule as $y_i = x_i(1 + \text{sign}(x_i)\xi)$, where $\{x_i\}_{i=1}^N$ and $\{y_i\}_{i=1}^N$ are the original and watermarked coefficients, respectively, and $\xi \in \Re^+$ is the watermark weighting factor. The binary watermark bits of 0 or 1 are embedded as

$$\begin{aligned} y_{i|1} &= (1 + \text{sign}(x_i)\xi)x_i, \quad 1 \text{ is embedded} \\ y_{i|0} &= (1 - \text{sign}(x_i)\xi)x_i, \quad 0 \text{ is embedded} \end{aligned} \tag{4}$$

Fig. 2. Watermark imperceptibility of the proposed scheme. (a) Host, (b) watermarked *Boat* image with $PSNR = 42.97$ *dB*, and (c) the difference between the host and watermarked images.

The watermarked contourlet coefficients of each block are then inverse transformed to obtain the watermarked image.

B. Watermark Extraction

A watermark decoder is designed by considering the statistics of the contourlet coefficients of images. It is noted that in the proposed decoder having access to the host image is not required and a blind watermark decoder is realized. It is known that the role of a decoder is to extract the hidden binary message from the observed image coefficients. In our proposed scheme, the contourlet coefficients of children and their corresponding parent are assumed to be distributed by the BVG model. In view of this, in order to extract the hidden message bits from the subband coefficients of images, an optimum decoder is built based on the bivariate Gaussian density function. To this end, for a subband with N observed coefficients in one scale, i.e., children coefficients $\{y_i\}_{i=1}^{N}$, and its corresponding parent in the preceding scale $\{y_j\}_{j=1}^{N}$, the maximum likelihood decision rule is formulated as [14]

$$P_{BVG}(\mathbf{y}|1) \underset{0}{\overset{1}{\gtrless}} P_{BVG}(\mathbf{y}|0), \tag{5}$$

in which the block coefficients for two consecutive scales are modeled by the zero-mean bivariate Gaussian PDF given by (7) and (8) as shown at the bottom of the next page. By inserting these statistical models into (5) and after some algebraic manipulations, a mathematical closed-form expression for the proposed decoder is derived as

$$\sum_{i,j=1}^{N} \frac{y_i}{y_j} \underset{0}{\overset{1}{\gtrless}} \sum_{i,j=1}^{N} \frac{\rho\left(1-(\xi \operatorname{sign}(y_i))^2\right)\sigma_i}{\sigma_j} \tag{6}$$

IV. Simulation Results

To evaluate the performance of the proposed watermark decoder, experiments are conducted using a number of gray scale test images, each having a size of 512×512 pixels [15]. The images are first partitioned into several non-overlapping blocks and those having the highest variances are selected for further processing. In particular, the selected blocks are decomposed by the contourlet transform with bi-orthogonal filters into three scales each having eight directional subbands. It is noted that the number of directional subbands in each scale should be the same; realizing a parent-children relation. To have both y_i and y_j to be of the same size, the parent subband is expanded by a factor of 2. To embed the hidden message bits in the finest scale, the subband having the highest energy is considered. It is noted that it is experimentally observed that embedding the watermark does not change the order of subbands with the highest energies. It is noted that, for a high robustness, watermark weighting factor ξ can be increased to a point where the watermark is still invisible. Accordingly, the optimum value for the weighting factor is experimentally found to be 0.5. To evaluate the watermark invisibility, the mean peak-signal-to-noise-ratio (PSNR) is computed for the host and marked images by taking the average over 20 runs with 50 different pseudo-random binary sequences as the watermark signal. When $\xi = 0.5$, the PSNR values for three of the test images, namely, *Barbara*, *Lena* and *Boat*, are 36.57, 44.45, and 42.97 dB, respectively. The imperceptibility of the watermarking scheme is illustrated in Fig. 2; demonstrating the host and watermarked *Boat* images, as well as the difference between the host and watermarked images. It should be noted that the PDFs of the host and marked images are assumed to be the same, i.e., embedding the watermark with small ξ does not change the distribution of the host image coefficients [2]. Therefore, the parameters of the BVG model can be estimated from the observation $\mathbf{y}$.

The performance of the proposed watermark decoder is measured by the bit error rate (BER). Fig. 3 shows the averaged BERs obtained using the proposed decoder and GG-based decoder in [3] over a number of images, when varying the watermark weighting factor ξ. From this figure, it is seen that the proposed BVG-based decoder provides lower BERs than the GG-based decoder does.

The performance of the proposed decoder in the contourlet domain is compared to that of the methods in [2]–[6] and [16]–[20] in presence of various attacks. Table I gives BER obtained using the proposed BVG-based decoder with a watermark having a length of 256 bits for a few of the test images, namely, *Barbara*, *Baboon*, and *Peppers*, under

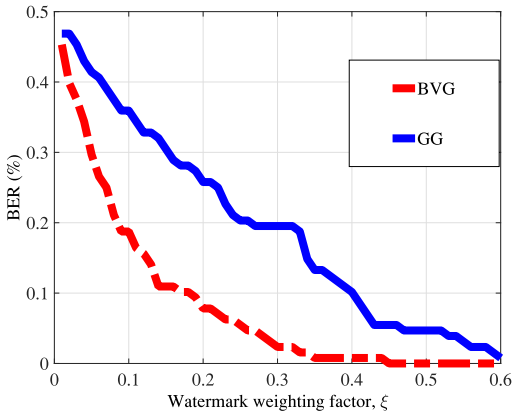

Fig. 3. BER (%) comparison between the proposed scheme and GG-based decoder in [3], averaged over a set of images.

TABLE I
BERs (%) Obtained Using the Proposed Scheme As Well As Those Obtained Using Other Schemes Under Various Attacks for Different Test Images. ($k = 256$ Bits, $PSNR = 42$ dB)

	JPEG ($QF = 11$)	AWGN $\sigma_n = 10$	Median filter 3×3
	Barbara		
Proposed	**0.75**	**0.14**	**0.85**
[5]	4.34	1.15	0.89
[20]	9.64	1.40	1.10
[17]	24.1	4.48	15.82
[18]	4.69	0.39	1.17
[19]	20.11	11.47	19.52
	Baboon		
Proposed	**0.46**	**0.0**	**0.31**
[5]	3.18	0.0	0.87
[20]	9.86	0.28	5.03
[17]	15.08	1.09	15.14
[18]	1.95	0.0	2.73
[19]	15.23	6.13	19.52
	Peppers		
Proposed	**2.70**	**0.0**	**0.0**
[5]	4.05	1.19	0.0
[20]	10.68	1.32	1.17
[17]	18.4	1.87	4.41
[18]	10.16	0.0	0.0
[19]	11.65	3.62	8.30

various attacks. The attacks considered in this experiment are JPEG compression with a quantization matrix indexed by a quality factor (QF) = 11, additive white Gaussian noise (AWGN) with mean zero and standard deviation $\sigma_n = 10$, and median filtering, for edge-preserving smoothening purpose, with window of size 3×3. It is seen from this table that the proposed BVG-based decoder provides considerably lower BERs in presence of different attacks; indicating its high robustness. Similar results have also been observed for the other test images.

TABLE II
Performance Comparison (BER (%)) for Various Watermark Decoders, When Watermarked Images Are Under Attacks. ($k = 128$ Bits)

	Proposed	[4]	[5]	[3]	[20]
	Barbara, PSNR=36 dB				
JPEG ($QF = 20$)	**0.0**	0.0	0.03	0.4	0.0
AWGN ($\sigma_n = 20$)	**0.13**	0.3	0.43	0.1	1.07
S&P ($p = 0.05$)	**0.06**	0.0	0.13	1.48	0.43
	Baboon, PSNR=39 dB				
JPEG ($QF = 20$)	**0.0**	0.0	0.0	1.89	0.0
AWGN ($\sigma_n = 20$)	**0.11**	0.13	0.27	0.30	1.48
S&P ($p = 0.05$)	**0.0**	0.0	0.18	2.89	0.89

TABLE III
Performance Comparison in Terms of BER for Various Watermarking Schemes, in Presence of Different Attacks. ($k = 64$ Bits, $PSNR = 42$ dB)

	Proposed	[4]	[16]	[20]	[8]
	Peppers				
JPEG ($QF = 5$)	**0.21**	0.32	0.78	-	6.25
Median filter 7×7	**0.0**	0.04	0.0	0.0	9.36
Median filter 9×9	**0.0**	0.05	3	4.62	51.56
S&P ($p = 0.08$)	**0.03**	0.03	-	0.40	2.51
	Baboon				
JPEG ($QF = 5$)	**0.0**	0.05	0.0	-	4.69
Median filter 7×7	**0.21**	0.42	4.88	3.81	12.50
Median filter 9×9	**0.33**	0.49	0.88	12.31	78.13
S&P ($p = 0.08$)	**0**	0.0	-	0.4	3.34

Table II gives BERs of the proposed decoder and those of the methods in [3]–[5] and [20], for an embedded hidden message having a length of $k = 128$ bits, under JPEG compression with $QF = 20$, AWGN with standard deviation $\sigma_n = 20$, and salt and pepper (S&P) noise with noise density $p = 0.05$, for *Barbara* and *Baboon* images. As seen from this table, the proposed watermark decoder provides lower BERs; indicating its higher robustness in presence of these attacks.

Table III gives BERs for the proposed decoder and the methods in [4], [8], [16], and [20], when $k = 64$ bits, under JPEG compression with $QF = 5$, median filter having a mask sizes of 7×7 and 9×9, and salt & pepper noise with $p = 0.08$, for *Peppers* and *Baboon* images. The results obtained in Table II clearly reveal that the proposed decoder is superior to other decoders in terms of robustness by providing lower BERs.

The performance of the BVG-based decoder in the contourlet domain is examined under the scaling attack and S&P noise. Tables IV and V give BER values of the proposed decoder and those yielded by the methods in [2] and [3], under these attacks. As observed from these tables, the BVG-based decoder is more robust against scaling attack and

$$P_{BVG}(\mathbf{y}|1) = \prod_{N} \exp\left[\frac{-1}{2(1-\rho^2)}\left\{\frac{\left(\frac{y_i}{(1+\text{sign}(y_i)\xi)}\right)^2}{\sigma_i^2} + \frac{y_j^2}{\sigma_j^2} - 2\rho\frac{\frac{y_i}{(1+\text{sign}(y_i)\xi)}}{\sigma_i}\frac{y_j}{\sigma_j}\right\}\right] \tag{7}$$

$$P_{BVG}(\mathbf{y}|0) = \prod_{N} \exp\left[\frac{-1}{2(1-\rho^2)}\left\{\frac{\left(\frac{y_i}{(1-\text{sign}(y_i)\xi)}\right)^2}{\sigma_i^2} + \frac{y_j^2}{\sigma_j^2} - 2\rho\frac{\frac{y_i}{(1-\text{sign}(y_i)\xi)}}{\sigma_i}\frac{y_j}{\sigma_j}\right\}\right] \tag{8}$$

TABLE IV
BER (%) OBTAINED USING THE PROPOSED DECODER AND THOSE IN [2] AND [3] UNDER SCALING ATTACK

	0.8			2		
	Proposed	[2]	[3]	**Proposed**	[2]	[3]
Barbara	**3.76**	4.11	10.39	**3.01**	3.35	8.28
Baboon	**5.19**	6.23	21.37	**0.79**	1.12	3.05
Couple	**1.67**	2.32	7.19	**0.77**	1.08	1.88
Bridge	**1.89**	2.69	7.85	**0.16**	0.21	0.47

TABLE V
BER (%) OBTAINED USING THE PROPOSED DECODER AND THOSE IN [2] AND [3] UNDER SALT & PEPPER NOISE ATTACK

	$p = 1\%$			$p = 3\%$		
	Proposed	[2]	[3]	**Proposed**	[2]	[3]
Barbara	**0.0**	1.53	3.28	**0.0**	2.30	4.18
Baboon	**0.0**	0.66	1.91	**0.0**	1.36	2.81
Couple	**0.22**	2.84	6.72	**1.34**	5.33	8.55
Bridge	**0.09**	1.81	5.43	**1.19**	4.08	7.27

TABLE VI
BER (%) OBTAINED USING THE PROPOSED DECODER AND THOSE IN [2] AND [17], UNDER CROPPING ATTACK. (MESSAGE LENGTH=256 BITS)

	5%			10%		
	Proposed	[2]	[17]	**Proposed**	[2]	[17]
Lena	**0.13**	0.5	1.83	**1.31**	3.4	5.92
Goldhill	**0.34**	1.8	2.84	**2.35**	6.1	6.53
Bridge	**0.30**	1.6	4.63	**2.60**	6.7	13.42
Peppers	**0.19**	0.8	6.58	**1.58**	5.1	10.48

S&P noise than the other methods; evidenced by the lower BERs. Table VI gives BER values obtained using the proposed decoder and those provided by the schemes in [2] and [17], when the test images are 5% or 10% cropped. The lower BER values seen from this table indicate the more robustness of the proposed BVG-based watermarking scheme as compared to the other methods in presence of cropping attack.

V. CONCLUSION

In this brief, an optimum watermark decoder has been proposed for multiplicative watermarking in the contourlet domain based on bivariate Gaussian model as a local prior for the coefficients of two consecutive scales. A mathematical closed-form expression for the proposed decoder has been derived for the watermark extraction by using the maximum likelihood criterion. The performance of the proposed decoder has been investigated through experiments and compared to that of a number of existing decoders. It has been demonstrated that the bivariate Gaussian-based watermark decoder provides a performance superior to those of the other decoders by achieving lower bit error rate values. The robustness of the proposed watermarking scheme has also been studied against compression, filtering, cropping, scaling and noise attacks, and shown to be higher than the other decoders.

REFERENCES

[1] H. Sadreazami, M. O. Ahmad, and M. N. S. Swamy, "A robust multiplicative watermark detector for color images in sparse domain," *IEEE Trans. Circuits Syst. II, Exp. Briefs*, vol. 62, no. 12, pp. 1159–1163, Dec. 2015.

[2] H. Sadreazami, M. O. Ahmad, and M. N. S. Swamy, "Multiplicative watermark decoder in contourlet domain using the normal inverse Gaussian distribution," *IEEE Trans. Multimedia*, vol. 18, no. 2, pp. 196–207, Feb. 2016.

[3] M. A. Akhaee, S. M. E. Sahraeian, and F. Marvasti, "Contourlet-based image watermarking using optimum detector in a noisy environment," *IEEE Trans. Image Process.*, vol. 19, no. 4, pp. 967–980, Apr. 2010.

[4] M. Amini, M. O. Ahmad, and M. N. S. Swamy, "A robust multibit multiplicative watermark decoder using a vector-based hidden Markov model in wavelet domain," *IEEE Trans. Circuits Syst. Video Technol.*, vol. 28, no. 2, pp. 402–413, Feb. 2018.

[5] M. Amini, M. O. Ahmad, and M. N. S. Swamy, "Digital watermark extraction in wavelet domain using hidden Markov model," *Multimedia Tools Appl.*, vol. 76, no. 3, pp. 3731–3749, 2017.

[6] S. Etemad and M. Amirmazlaghani, "A new multiplicative watermark detector in the contourlet domain using t Location-Scale distribution," *Pattern Recognit.*, vol. 77, pp. 99–112, May 2018.

[7] H. Song, S. Yu, X. Yang, L. Song, and C. Wang, "Contourlet-based Image adaptive watermarking," *Signal Process. Image Commun.*, vol. 23, no. 3, pp. 162–178, 2008.

[8] N. Bi, Q. Sun, D. Huang, Z. Yang, and J. Huang, "Robust image watermarking based on multiband wavelets and empirical mode decomposition," *IEEE Trans. Image Process.*, vol. 16, no. 8, pp. 1956–1966, Aug. 2007.

[9] T. M. Ng and H. K. Garg, "Maximum-likelihood detection in DWT domain image watermarking using Laplacian modeling," *IEEE Signal Process. Lett.*, vol. 12, no. 4, pp. 285–288, Apr. 2005.

[10] M. Rabizadeh, M. Amirmazlaghani, and M. Ahmadian-Attari "A new detector for contourlet domain multiplicative image watermarking using Bessel K form distribution," *J. Vis. Commun. Image Represent.*, vol. 40, pp. 324–334, Oct. 2016.

[11] H. Sadreazami, M. O. Ahmad, and M. N. S. Swamy, "Contourlet domain image modeling by using the alpha-stable family of distributions," in *Proc. IEEE Int. Symp. Circuits Syst. (ISCAS)*, Melbourne, VIC, Australia, 2014, pp. 1288–1291.

[12] D. D.-Y. Po and M. N. Do, "Directional multiscale modeling of images using the contourlet transform," *IEEE Trans. Image Process.*, vol. 15, no. 6, pp. 1610–1620, Jun. 2006.

[13] R. A. Johnson and D. W. Wichern, *Applied Multivariate Statistical Analysis*, 1st ed. Englewood Cliffs, NJ, USA: Prentice-Hall, 1982.

[14] S. M. Kay, *Fundamentals of Statistical Signal Processing, Volume II: Detection Theory*, 1st ed. Englewood Cliffs, NJ, USA: Prentice-Hall, 1998.

[15] *Online Image Database.* Accessed: Jan. 2018. [Online]. Available: http://decsai.ugr.es/cvg/dbimagenes/index.php

[16] M. A. Akhaee, S. M. E. Sahraeian, B. Sankur, and F. Marvasti, "Robust scaling-based image watermarking using maximum-likelihood decoder with optimum strength factor," *IEEE Trans. Multimedia*, vol. 11, no. 5, pp. 822–833, Aug. 2009.

[17] M. Hamghalam, S. Mirzakuchaki, and M. A. Akhaee, "Geometric modeling of the wavelet coefficients for image watermarking using optimum detector," *IET Image Process.*, vol. 8, no. 3, pp. 162–172, 2014.

[18] X. Zhu, J. Ding, H. Dong, K. Hu, and X. Zhang, "Normalized correlation-based quantization modulation for robust watermarking," *IEEE Trans. Multimedia*, vol. 16, no. 7, pp. 1888–1904, Nov. 2014.

[19] M. Hamghalam, S. Mirzakuchaki, and M. A. Akhaee, "Vertex angle image watermarking with optimal detector," *Multimedia Tools Appl.*, vol. 74, no. 9, pp. 3077–3098, 2015.

[20] E. Nezhadarya, Z. J. Wang, and R. K. Ward, "Robust image watermarking based on multiscale gradient direction quantization," *IEEE Trans. Inf. Forensics Security*, vol. 6, no. 4, pp. 1200–1213, Dec. 2011.

[21] H. Sadreazami, M. O. Ahmad, and M. N. S. Swamy, "A robust quantization-based image watermarking scheme in the wavelet-based contourlet domain," in *Proc. IEEE Can. Conf. Elect. Comput. Eng. (CCECE)*, Vancouver, BC, Canada, 2016, pp. 1–4.